Estimation of Q-Factors and Resonant Frequencies

Kevin J. Coakley, Jolene D. Splett, Michael D. Janezic, *Senior Member, IEEE*, and Raian F. Kaiser

***Abstract*—We estimate the quality factor Q and resonant frequency f_0 of a microwave cavity based on observations of a resonance curve on an equally spaced frequency grid. The observed resonance curve is the squared magnitude of an observed complex scattering parameter. We characterize the variance of the additive noise in the observed resonance curve parametrically. Based on this noise characterization, we estimate Q and f_0 and other associated model parameters using the method of weighted least squares (WLS). Based on asymptotic statistical theory, we also estimate the one-sigma uncertainty of Q and f_0. In a simulation study, the WLS method outperforms the 3-dB method and the Estin method. For the case of measured resonances, we show that the WLS method yields the most precise estimates for the resonant frequency and quality factor, especially for resonances that are undercoupled. Given that the resonance curve is sampled at a fixed number of equally spaced frequencies in the neighborhood of the resonant frequency, we determine the optimal frequency spacing in order to minimize the asymptotic standard deviation of the estimate of either Q or f_0.**

***Index Terms*—Cylindrical cavity, experimental design, microwave, noise characterization, optimal frequency spacing, quality factor, resonance curve, resonant frequency.**

I. Introduction

In THIS study, we characterize the frequency-dependent additive noise in measured microwave cavity resonance curves and estimate the quality factor Q and resonant frequency f_0 of the microwave cavity. The data used are the squared magnitudes of the observed values of frequency-dependent complex scattering parameters $|S_{21}|^2$.

The resonance curve parameters Q and f_0 can be estimated from the observed values of $|S_{21}|^2$ using either the 3-dB or the Estin method [1]. The Estin method is an example of a resonance curve area (RCA) method [2]. In these approaches, the estimated resonant frequency is the frequency at which the resonance curve reaches its maximum value. Hence, the estimated resonant frequency is constrained to take discrete values. Further, neither the 3-dB nor the Estin method exploits knowledge about frequency-dependent additive noise in the data. In related work, Petersan and Anlage [3] demonstrated that the method of least squares (LS) provides superior estimates of Q and f_0 when compared to the 3-dB method and to the related RCA method for a similar resonance curve problem. However, for cases where the variance of the additive noise varies with frequency, the method of LS is suboptimal. Further, the LS method does not provide an estimate of the covariance of the estimated model parameters.

Manuscript received April 1, 2002; revised September 23, 2002.

K. J. Coakley and J. D. Splett are with the Statistical Engineering Division, National Institute of Standards and Technology, Boulder, CO 80305 USA (e-mail: kevin.coakley@nist.gov; jolene.splett@nist.gov).

M. D. Janezic and R. F. Kaiser are with the RF Technology Division, National Institute of Standards and Technology, Boulder, CO 80305 USA (e-mail: michael.janezic@nist.gov; raian.kaiser@nist.gov).

Digital Object Identifier 10.1109/TMTT.2003.808578

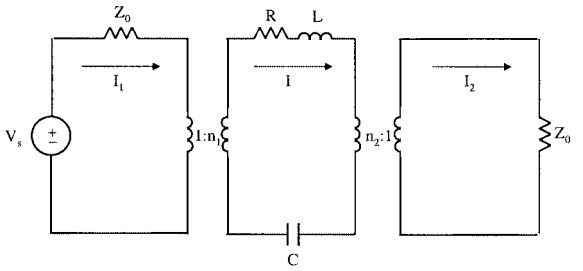

Fig. 1. Resonant cavity equivalent circuit model.

Here, we present a new method to estimate Q and f_0 that accounts for frequency-dependent additive noise. We characterize the frequency-dependent noise in the measured resonance curve in terms of a parametric model with two parameters. In the statistical literature, such an approach is known as variance function estimation [4]. In our model, one parameter corresponds to a noise floor, while the other parameter represents the frequency-dependent part of the noise. Based on the estimated variance function parameters, we estimate the resonance curve parameters (including Q and f_0) using the weighted least squares (WLS) method. Due to the sensitive nature of this optimization problem, we take special care to ensure that we find (or very nearly find) the global minimum of the objective function that we seek to minimize. In particular, instead of starting our optimization algorithm from just one set of initial guesses for the model parameters, we perform the optimization algorithm for each of many randomly selected initial guesses.

Based on the estimated variance function parameters and estimated resonance curve model parameters, we estimate the one-sigma random errors of Q and f_0 using asymptotic statistical theory. In our experiments, the resonance curve is sampled at 201 equally spaced frequencies in the neighborhood of the resonant frequency. We compute the asymptotic standard deviation of the Q and f_0 estimates as a function of the frequency spacing df, the model parameters that characterize the resonance curve, and the additive noise. For optimal estimation of Q, using our experimental data, $\Delta = Q(f_{\max}/f_0 - 1) \approx 2.6$, where $f_{\max}$ is the largest frequency. For optimal estimation of f_0, $\Delta \approx 0.6$.

II. Resonance Curve Model

We model a two-port cylindrical cavity with the equivalent circuit shown in Fig. 1 [5], [6]. In particular, we are interested in measuring an undercoupled cavity, with a high quality factor, operating near resonance. In this case, we assume that the resistances and self-inductances of the coupling loops are negligible [5]. We employ two ideal transformers to model the coupling

loops that excite the cylindrical cavity. We use a series inductor (L), capacitor (C), and resistor (R) to model the cylindrical cavity. An impedance-matched source is connected to port one of the cavity while an impedance-matched load is connected to port two. Note that the source and load can be interchanged without loss of generality.

We define $T(f)$ as the transmission loss through the cylindrical cavity

$$T(f) = \frac{P_{\text{in}}}{P_L} \tag{1}$$

where f is the frequency, P_{in} is the maximum power delivered to a matched load connected at port one, and P_L is the maximum power delivered to the load at port two [5]. Solving for P_{in} and P_L we find

$$P_{\text{in}} = I_1 I_1^* Z_0 = \frac{V_s^2}{4Z_0} \tag{2}$$

and

$$\begin{aligned} P_L &= I_2 I_2^* Z_0 \\ &= \frac{V_s^2}{Z_0} \frac{\beta_1 \beta_2}{(1+\beta_1+\beta_2)^2 + Q_0^2 \left(\frac{f}{f_0} - \frac{f_0}{f}\right)^2} \end{aligned} \tag{3}$$

where

$$\beta_1 = \frac{n_1^2 Z_0}{R} \tag{4}$$

and

$$\beta_2 = \frac{n_2^2 Z_0}{R}. \tag{5}$$

In (3), the resonant frequency f_0 is defined as

$$f_0^2 = \frac{1}{4\pi^2 LC} \tag{6}$$

and the unloaded quality factor Q_0 is

$$Q_0 = \frac{2\pi f_0 L}{R}. \tag{7}$$

Substituting (2) and (3) into (1) we obtain

$$T(f) = \frac{4\beta_1\beta_2}{(1+\beta_1+\beta_2)^2 + Q_0^2 \left(\frac{f}{f_0} - \frac{f_0}{f}\right)^2}. \tag{8}$$

At resonance $(f = f_0)$, the transmission loss reduces to

$$T(f_0) = \frac{4\beta_1\beta_2}{(1+\beta_1+\beta_2)^2}. \tag{9}$$

Taking the ratio of $T(f_0)/T(f)$ we obtain

$$\frac{T(f_0)}{T(f)} = 1 + \frac{Q_0^2 \left(\frac{f}{f_0} - \frac{f_0}{f}\right)^2}{(1+\beta_1+\beta_2)^2}. \tag{10}$$

Note that, in practice, the unloaded quality factor Q_0 is larger than the measured quality factor Q due to the effects of the coupling loops

$$Q_0 = Q(1+\beta_1+\beta_2). \tag{11}$$

However, if we reduce the coupling level so that the cylindrical cavity is very undercoupled ($\beta_1 \ll 1$ and $\beta_2 \ll 1$), we can neglect the coupling factors β_1 and β_2 and rewrite (10) as

$$T(f) = \frac{T(f_0)}{1 + Q^2 \left(\frac{f}{f_0} - \frac{f_0}{f}\right)^2} \approx \frac{T(f_0)}{1 + Q_0^2 \left(\frac{f}{f_0} - \frac{f_0}{f}\right)^2} \tag{12}$$

with the assumption that the measured quality factor Q is approximately Q_0. (If coupling cannot be ignored, see [7] for methods of calculating β_1 and β_2.)

At the kth frequency, we model the measured resonance curve as

$$T_m(f_k) = \frac{T(f_0)}{1 + Q^2 \left(\frac{f_k}{f_0} - \frac{f_0}{f_k}\right)^2} + \text{BG} + \epsilon(f_k) \tag{13}$$

where $T_m(f_k) = |S_{21}(f_k)|^2$ represents the observed measurement, $T(f_k)$ denotes the true value or "noise-free" measurement, BG is a noise floor, and $\epsilon(f_k)$ is additive noise with an expected value of zero and variance $\sigma^2_{\epsilon(f_k)}$. The model parameters form a four-vector, $\vec{\theta} = (\theta_1, \theta_2, \theta_3, \theta_4) = (T(f_0), Q, f_0, \text{BG})$. For the observed data, we model the variance of the additive noise as

$$\text{VAR}[\epsilon(f_k)] = \sigma^2_{\epsilon(f_k)} = \frac{\gamma_1^2}{1 + Q^2 \left(\frac{f_k}{f_0} - \frac{f_0}{f_k}\right)^2} + \gamma_2^2 \tag{14}$$

where γ_1 and γ_2 correspond to the frequency-dependent noise and the noise floor, respectively. In Appendix C, we prove that our variance function model (14) is exact for the case where the additive noise in the measurement of the real part of S_{21} and the additive noise in the measurement of the imaginary part of S_{21} are statistically independent realizations of the same Gaussian process. In our proof, we assume that the expected values of the additive noise realizations are zero.

A. Parameter Estimation

Suppose we measure the resonance curve at M distinct frequencies and estimate the model parameters by minimizing a weighted sum of M squared residuals

$$L = \sum_{k=1}^{M} w_k \left[T_m(f_k)) - \hat{T}_m(f_k)\right]^2. \tag{15}$$

If the weights w_k are all equal, minimization of L yields the LS estimate of $\vec{\theta}$. If the kth weight is set to the reciprocal of the (estimated) variance of $T_m(f_k)$, i.e., $w_k = 1/\text{VAR}[T_m(f_k)]$, then minimization of L yields the WLS estimate of $\vec{\theta}$.

We assume that additive noise realizations are statistically independent. Given the parameters which characterize the resonance curve $\vec{\theta}$ and the variance of the additive noise, asymptotic theory [8] predicts the covariance of the parameter estimates. From one curve, the predicted covariance is

$$\widehat{\text{COV}}(\hat{\vec{\theta}}) = (B^T V^{-1} B)^{-1} \tag{16}$$

where the elements of the diagonal matrix V are

$$V_{kk} = \text{VAR}\left[T_m(f_k)\right] \tag{17}$$

and

$$B_{kj} = \frac{\partial \langle T_m(f_k) \rangle}{\partial \theta_j}. \tag{18}$$

Thus, the predicted asymptotic variance of the mth parameter estimated from a resonance curve is

$$\sigma^{*^2}_{\theta_m} = (B^T V^{-1} B)^{-1}_{mm}. \tag{19}$$

Alternatively, the asymptotic standard error (ASE) of the estimate of θ_m is

$$\sigma^*_{\theta_m} = \sqrt{(I^{-1})_{mm}} \tag{20}$$

where

$$I_{ij} = \sum_{k=1}^{M} \frac{1}{\mathrm{VAR}[T_m(f_k)]} \frac{\partial \langle T_m(f_k) \rangle}{\partial \theta_i} \frac{\partial \langle T_m(f_k) \rangle}{\partial \theta_j}. \tag{21}$$

The ASE can be thought of as an approximation for the standard deviation of the parameter. As the signal-to-noise ratio (SNR) of the data increases, the accuracy of this approximation improves in general. For more discussion of asymptotic properties of estimates of nonlinear WLS, see [8].

B. Computational Details

The algorithm for estimation of Q and f_0 has four steps.

Step 1) Compute $\hat{Q}$ using the Estin method [1]. (See Appendix A.)

Step 2) Use $\hat{Q}$ from the Estin method as a starting value in the nonlinear fitting algorithm that computes unweighted LS estimates of the model parameters. The background parameter BG is constrained to be positive by expressing it as the squared value of the appropriate parameter in the model.

Step 3) Estimate the variance function and weights based on the "binned" squared residuals by the method of LS. Frequency bins were determined by dividing the entire frequency range of the resonance curve into 40 equal sections. The variance estimates were adjusted upward by a degree of freedom factor of $201/197$.

Although the variance is modeled using γ_1^2 and γ_2^2 to ensure a positive variance estimate, the optimization code searches for a solution in the unconstrained γ_1 and γ_2 space. We report $|\hat{\gamma}_1|$ and $|\hat{\gamma}_2|$.

A typical variance function is shown in Fig. 2(c). The vertical axis displays the fractional residuals, which are absolute residuals divided by $\hat{\theta}_1$, and the horizontal dashed line near the bottom of the plot represents the fractional background level, $\hat{\gamma}_2/\hat{\theta}_1$. Fig. 2(d) displays the same data when residuals are assigned to frequency bins and the average fractional residual is computed for each bin.

Step 4) Use the *unweighted* LS parameter estimates as starting values in the nonlinear fitting algorithm that computes *weighted* LS parameter estimates. The weights used in the nonlinear fit are derived from the variance function estimated in step 3.

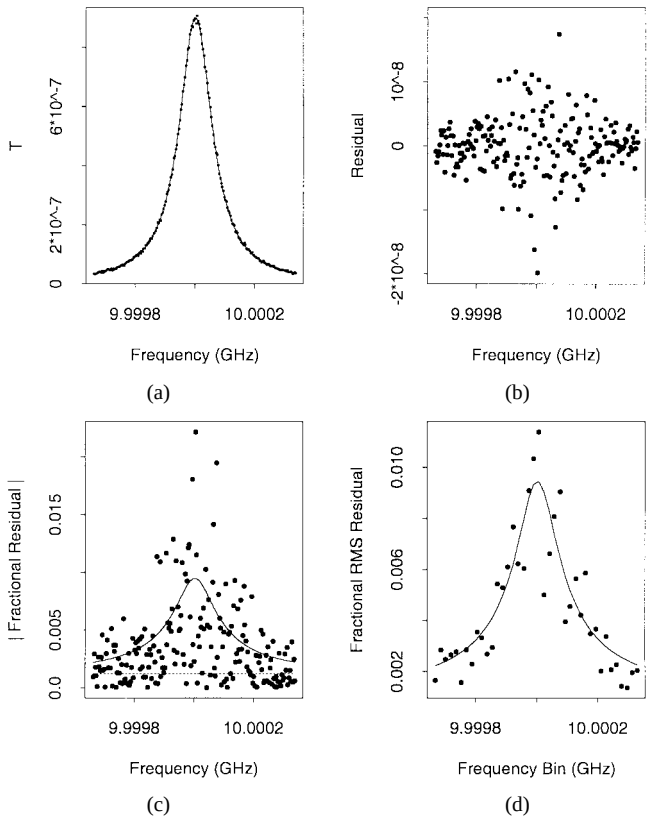

Fig. 2. (a) An observed and predicted (from WLS fit) resonance curve. (b) Raw residuals. (c) Fractional residuals (absolute residuals divided by $\hat{\theta}_1$). (d) Binned fractional rms residuals versus frequency. In (a) and (d), model predictions are shown as solid lines.

The nonlinear fitting routine used to determine the LS and WLS parameter estimates minimizes a general, unconstrained objective function using the analytic gradient and Hessian of the objective function [9].

The objective function was minimized for each of 250 randomly generated initial parameter values. The final parameter estimates are those that yield the smallest value of the objective function. If only one set of initial parameter values is used, the objective function may converge to a local minimum rather than the global minimum.

The same nonlinear fitting routine used to compute LS and WLS parameter estimates was also used to estimate the variance function parameters. Again, we experienced convergence problems, so random initial parameter values were used.

III. Experimental Study

In our study, we employed a cylindrical cavity resonator, shown in Fig. 3. The cavity was nominally 450 mm long and 60 mm in diameter, and it was composed of a helically wound cylindrical waveguide terminated by two endplates. Both of the gold-plated endplates were optically polished. One endplate was fixed on the top of the cylindrical cavity, while the bottom endplate, with a slightly smaller diameter than that of the cylindrical waveguide, traveled over a range of 25 mm through the use of a motorized micrometer drive. Movement of the bottom endplate allowed for tuning of the cavity resonant frequency.

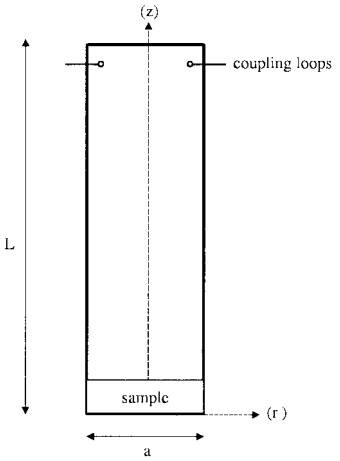

Fig. 3. Cylindrical cavity in the "sample loaded" state.

As in [10] and [11], use of a helical waveguide attenuated many of the undesired resonant modes while allowing the TE_{01n} cavity modes to propagate. Our particular helical waveguide consisted of two copper wires embedded in epoxy surrounded by a fiberglass cylinder. Although the helical waveguide lowered the quality factor of the cavity slightly, it also eliminated many of the unwanted resonant modes. Thus, the advantages of using the helical waveguide outweighed its associated disadvantages.

Near the top of the cylindrical waveguide section were two coupling loops, extending from two coupling holes located on opposite sides of the cylindrical waveguide. In order to excite a resonance in the cylindrical cavity, each coupling loop was connected to an automatic network analyzer via a coaxial transmission line. Cavity coupling was altered by changing the extent that the coupling loops protruded into the cavity. In particular, we kept the resonant peak amplitude below -50 dB so that the losses due to the coupling loops were negligible.

We operated the cylindrical cavity in two states, "air" and "sample loaded." The "air" state refers to the cavity without a sample present, while the "sample loaded" state refers to the cavity with a dielectric sample on the bottom endplate. We adjusted the cylindrical cavity length to obtain a resonant frequency near 10 GHz for each cavity state. For each cavity state, 30 resonance curves were collected at two different frequency spacings df. Each resonance curve was made up of 201 equally spaced points, and we performed 512 averages on each resonance curve to reduce the level of noise. For each curve, we estimated $\hat{Q}$ and $\hat{f}_0$ by various methods. Fig. 4 displays the estimates of Q and f_0 for each of the 30 experimental curves corresponding to the "sample loaded" state. The binned fractional root-mean-square (rms) residuals and the estimated variance functions are shown in Fig. 5 for the 30 "sample loaded" resonance curves.

Tables I and II display mean estimates of Q and f_0 and their associated standard deviations (shown in parentheses) for the various methods. For each curve, we estimated the ASE based on the parameter estimates and (20). The WLS method yields estimates with the lowest variability.

For 30 realized data sets, a 95% two-sided confidence interval for σ is $(0.7964\hat{\sigma}, 1.3443\hat{\sigma})$. Thus, the sampling error is not

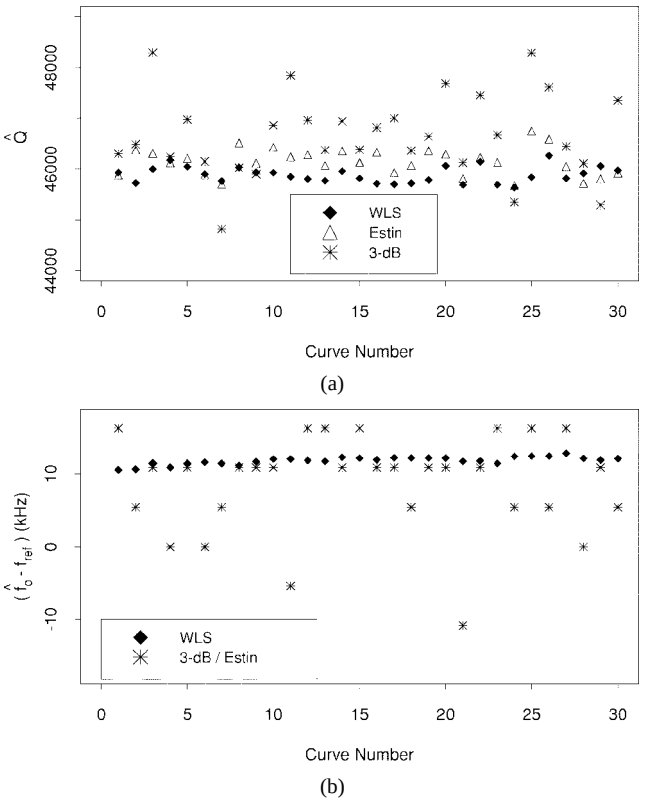

Fig. 4. Estimated values of: (a) Q and (b) $f_0 - f_{\mathrm{ref}}$ ($f_{\mathrm{ref}} = 10$ GHz) for each of 30 experimental curves corresponding to the "sample loaded" state where $\Delta = 2.4396$.

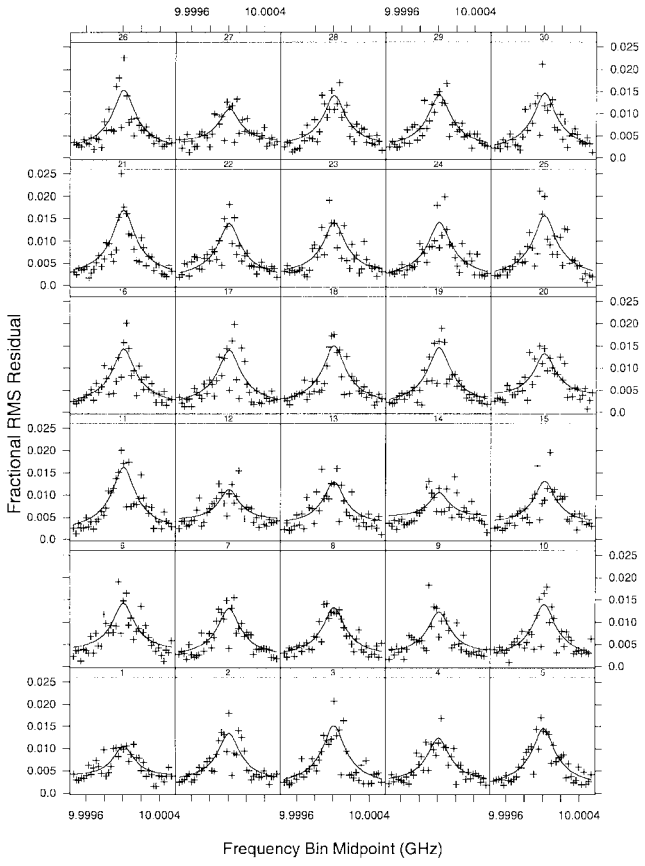

Fig. 5. Predicted (lines) and observed variance functions for 30 observed resonance curves corresponding to the "sample loaded" state.

TABLE I
STATISTICAL PROPERTIES OF Q ESTIMATES COMPUTED FROM REAL DATA INCLUDING: THE MEAN OF $\hat{Q}$, STANDARD ERROR OF THE MEAN (SHOWN IN PARENTHESES), AND THE STANDARD ERROR OF $\hat{Q}$. FOR THE WLS METHOD, WE LIST THE MEAN ESTIMATE OF $\sigma^*_{\hat{Q}}$, THE ASE OF $\hat{Q}$ (20), AND ITS ASSOCIATED STANDARD ERROR

Cavity State	df (Hz)	Estin	3-dB	LS	WLS	$\hat{\sigma}^*_{\hat{Q}}$
air	3400	74335(45)	75051(140)	74119(61)	74081(44)	
		246	766	334	241	238(3)
	1000	75150(90)	75406(117)	74143(63)	74153(55)	
		491	643	347	304	528(5)
sample loaded	5400	46143(49)	46659(150)	45885(40)	45888(29)	
		270	823	218	161	206(3)
	1500	47225(70)	47303(110)	46029(53)	46020(48)	
		381	605	292	263	483(5)

TABLE II
STATISTICAL PROPERTIES OF f_0 ESTIMATES COMPUTED FROM REAL DATA INCLUDING: THE MEAN OF $\hat{f}_0 - f_{\rm ref}$ ($f_{\rm ref} = 10$ GHz), STANDARD ERROR OF THE MEAN (SHOWN IN PARENTHESES), AND THE STANDARD ERROR OF $\hat{f}_0$. FOR THE WLS METHOD, WE LIST THE MEAN ESTIMATE OF $\sigma^*_{\hat{f}_0}$, THE ASE OF $\hat{f}_0$ (20), AND ITS ASSOCIATED STANDARD ERROR

Cavity State	df (Hz)	Estin, 3-dB $\hat{f}_0 - f_{ref}$ (Hz)	LS $\hat{f}_0 - f_{ref}$ (Hz)	WLS $\hat{f}_0 - f_{ref}$ (Hz)	$\hat{\sigma}^*_{\hat{f}_0}$
air	3400	2365(651)	1424(81)	1458(79)	
		3565	444	435	125(2)
	1000	-2381(653)	-3249(119)	-3245(119)	
		3578	654	650	79(0.8)
sample loaded	5400	8696(1239)	11534(94)	11845(98)	
		6785	517	537	280(5)
	1500	8530(960)	9710(45)	9751(44)	
		5258	249	239	182(2)

large enough to explain the discrepancy between the empirical standard deviation of the Q estimates and the estimated ASE at $df = 1000$ Hz and 1500 Hz.

The asymptotic standard error of $\hat{f}_0$ is much smaller than the estimated standard deviation of $\hat{f}_0$ computed from the 30 resonance curves. We attribute this discrepancy to systematic drift of the resonant frequency during the experiment. The variability of the Estin/3-dB estimate is much larger than the variability of the LS and WLS estimates.

IV. THEORETICAL STUDIES

A. Optimal Frequency Spacing

Based on $\vec{\theta}$ and $\vec{\gamma}$, we compute asymptotic standard errors $\sigma^*_{\hat{Q}}$ and $\sigma^*_{\hat{f}_0}$ using (14)–(21). In our first study, we equate the resonance frequency to the model parameters of the corresponding mean values computed from the observed resonance curves (Table III). In all cases, the resonance curve is sampled at 201 equally spaced frequencies. We define

$$\Delta = Q\frac{f_{\max} - f_0}{f_0} \tag{22}$$

where $f_{\max} = f_0 + 100df$. In Fig. 6, we show the fractional asymptotic standard error (ASE) of the estimates of Q and f_0 as a function of df. The optimal values of df for estimation of Q and f_0 are listed in Table IV.

TABLE III
PARAMETER VALUES USED IN THE SIMULATION $f_{\rm ref} = 10$ GHz

Parameter	"sample loaded" $df = 5400$ Hz	"air" $df = 3400$ Hz
$\theta_1 \times 10^9$	446.4	894.3
θ_2	45888	74081
$\theta_3 - f_{ref}$ (Hz)	11845	1458
$\theta_4 \times 10^9$	0.20	0.28
$\gamma_1 \times 10^9$	6.37	8.80
$\gamma_2 \times 10^9$	0.95	1.21

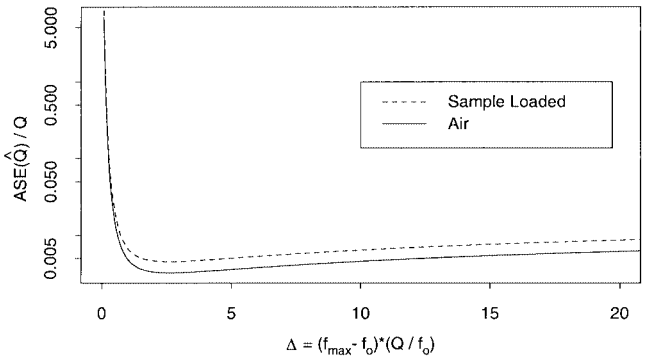

(a)

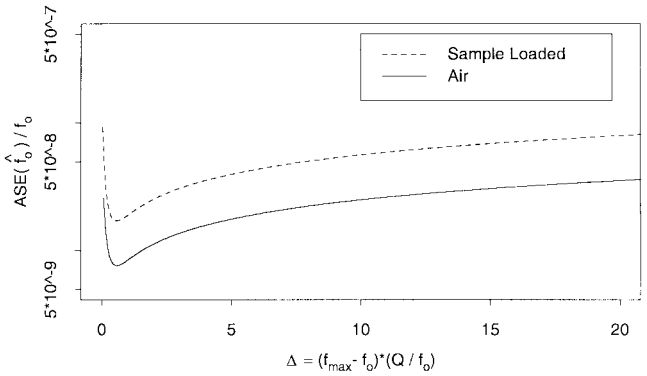

(b)

Fig. 6. Fractional asymptotic standard errors of: (a) $\hat{Q}$ and (b) $\hat{f}_0$ where model parameters are equated to estimated values from real data. Values of Q are 74 081.32 and 45 888.34 for "air" and "sample loaded" cavity states, respectively.

TABLE IV
THEORETICAL ASES (20) OF $\hat{Q}$ AND $\hat{f}_0$ BASED ON DATA SIMULATED USING TABLE III PARAMETER VALUES

Parameter Estimate	Cavity State	df (Hz)	Δ	Theoretical ASE
$\hat{Q}$	air	1000	0.7482	516.181
		3400	2.5262	240.030
		3500[a]	2.6003	239.940
	sample loaded	1500	0.6929	501.346
		5400	2.4826	208.045
		5700[a]	2.5743	207.924
$\hat{f}_0$	air	1000	0.7482	78.2 Hz
		3400	2.5262	126 Hz
		820[a]	0.6001	76.5 Hz
	sample loaded	1500	0.6929	173.6 Hz
		5400	2.4826	281.1 Hz
		1400[a]	0.6011	171.7 Hz

[a] optimal

TABLE V
STATISTICAL PROPERTIES OF ESTIMATES OF Q COMPUTED FROM SIMULATION DATA INCLUDING: BIAS OF THE ESTIMATE, STANDARD ERROR OF THE BIAS (SHOWN IN PARENTHESES), AND THE STANDARD ERROR OF THE ESTIMATE. THE MEAN OF THE ESTIMATED VALUE OF ASE, $\widehat{\text{ASE}}$, IS SHOWN FOR THE WLS METHOD

Q	Spacing (Hz)	3-dB	Estin	WLS	$\widehat{\text{ASE}}$	ASE
74081	1000	1381(22)	1175(15)	176(10)		
	($\Delta = 0.7408$)	701	475	332	523	517
	3400	706(25)	183(11)	32(7)		
	($\Delta = 2.5188$)	804	339	209	234	235
	6800	279(26)	-215(18)	12(8)		
	($\Delta = 5.0375$)	831	562	253	250	259
45888	1500	1385(18)	1169(13)	173(10)		
	($\Delta = 0.6883$)	581	421	314	505	499
	5400	672(21)	220(9)	28(6)		
	($\Delta = 2.4780$)	652	286	179	202	203
	10800	344(22)	42(16)	12(7)		
	($\Delta = 4.9559$)	693	508	218	215	223

TABLE VI
STATISTICAL PROPERTIES OF f_0 ESTIMATES COMPUTED FROM SIMULATION DATA INCLUDING: BIAS OF THE ESTIMATE, STANDARD ERROR OF THE BIAS (SHOWN IN PARENTHESES), AND THE STANDARD ERROR OF THE ESTIMATE. THE MEAN OF THE ESTIMATED VALUE OF ASE, $\widehat{\text{ASE}}$, IS SHOWN FOR THE WLS METHOD

Q	Spacing (Hz)	3-dB/Estin (Hz)	WLS (Hz)	$\widehat{\text{ASE}}$ (Hz)	ASE (Hz)
74081	1000	-156(104)	2(2)		
	($\Delta = 0.7408$)	3300	75	78	77
	3400	-17(12)	5(4)		
	($\Delta = 2.5188$)	3808	124	122	124
	6800	7(1324)	4(6)		
	($\Delta = 5.0375$)	4188	178	166	175
45888	1500	-368(193)	3(5)		
	($\Delta = 0.6883$)	6114	166	173	171
	5400	54(223)	11(9)		
	($\Delta = 2.4780$)	7044	275	271	276
	10800	130(242)	10(13)		
	($\Delta = 4.9559$)	7655	395	371	389

B. Monte Carlo Study

We simulate data similar to observed data for both cavity states. In Tables V and VI, we compare the performance of the various methods for estimating Q and f_0. In Table VII, we list the statistical properties of our variance function parameter estimates. For the lowest frequency spacing, the standard errors of the Q estimates are lower than what is predicted by asymptotic theory. For the other frequency spacings, the asymptotic theory predicts the standard error of the Q estimate well. For all frequencies, the standard error of the f_0 estimate is well predicted by asymptotic theory.

V. SUMMARY

The frequency-dependent additive noise in measured microwave cavity resonance was characterized. The observed data were the squared magnitude of a frequency-dependent complex scattering parameter $|S_{21}|^2$. Based on a parametric model for the additive noise of the observed resonance curve, Q and f_0 and other associated model parameters were estimated using the method of WLS. Asymptotic statistical theory was used to estimate the one-sigma uncertainty of Q and f_0. We found that the WLS method outperformed the 3-dB method and the Estin method (an example of the RCA method). For real data, the WLS method yielded the most precise estimates. An advantage to using the WLS method is that Q and f_0 estimates have less variability than the other methods even for "noisy" resonance curves. ("Noisy" data can occur due to inadequate signal averaging and/or low coupling.) For one observed resonance curve, the 3-dB method does not provide an associated uncertainty for Q and f_0 whereas the WLS method does.

TABLE VII
TRUE VARIANCE FUNCTION PARAMETERS IN SIMULATION STUDY AND MEAN VALUES OF ESTIMATED VARIANCE FUNCTION PARAMETERS. STANDARD ERRORS ARE SHOWN IN PARENTHESES

Q	$\gamma_1 \times 10^9$	$\gamma_2 \times 10^9$	df (Hz)	$\widehat{\gamma_1} \times 10^9$	$\widehat{\gamma_2} \times 10^9$
74081	8.7797	1.2058	1000	8.15(4)	2.19(5)
			3400	8.34(3)	1.43(2)
			6800	8.12(5)	1.34(2)
45888	6.3741	0.94678	1500	5.88(3)	1.68(4)
			5400	6.06(3)	1.08(2)
			10800	5.91(3)	1.03(1)

Given that the resonance curve was sampled at a fixed number of equally spaced frequencies in the neighborhood of the resonant frequency, we determined the optimal frequency spacing in order to minimize the asymptotic standard deviation of the estimate of either Q or f_0. For optimal estimation of Q, with our experimental data, $\Delta = Q(f_{\max}/f_0 - 1) \approx 2.6$, where $f_{\max}$ is the largest frequency. For optimal estimation of f_0, $\Delta \approx 0.6$. The fractional uncertainty of f_0 is smaller than the fractional uncertainty of Q when mode interference is neglected.

APPENDIX A
ESTIN METHOD

If additive noise and background are neglected, the resonance curve model can be written as

$$T_m(f_k) = \frac{T(f_0)}{1 + Q^2\left(\frac{f_k}{f_0} - \frac{f_0}{f_k}\right)^2}.$$

A good approximation for high Q values is

$$2Q\left(\frac{f_k - f_0}{f_0}\right) \cong \left|\frac{T_m(f_0)}{T_m(f)}\right|^{1/2}.$$

At the kth frequency, define

$$x_k = \frac{2(f_k - \hat{f}_0)}{\hat{f}_0},$$

and

$$y_k = \left|\frac{T_m(f_0)}{T_m(f_k)}\right|^{1/2}.$$

Define

$$\hat{y}_k = \alpha_1 x_k + \alpha_2.$$

The values of α_1 and α_2 that minimize

$$\sum |y_k - \hat{y}_k|^2$$

are called $\hat{\alpha}_1$ and $\hat{\alpha}_2$. The Estin estimator of Q is $\hat{\alpha}_1$ [1].

APPENDIX B
THE 3-dB METHOD

Define

$$r_{\rm dB}(\Delta f) = 10\log_{10}\left[\frac{T(\hat{f}_0)}{T(\hat{f}_0+\Delta f)}\right].$$

Define Δf^+ to be the positive value of Δf such that $r_{\rm dB}(\Delta f^+) = 3$, and Δf^- to be the negative value of Δf such that $r_{\rm dB}(\Delta f^-) = 3$. According to the 3-dB method, we have

$$\hat{Q} = \frac{\hat{f}_0}{[\Delta f^+ - \Delta f^-]}.$$

If there is no measurement at the frequencies corresponding to $r_{\rm dB}(\Delta f^+) = 3$ or $r_{\rm dB}(\Delta f^-) = 3$, Δf^+ or Δf^- is estimated by a linear interpolation method.

APPENDIX C
VARIANCE FUNCTION DERIVATION: SPECIAL CASE

The quantity $T(f_k)$ is the sum of the squared real and imaginary components of the complex scattering parameter $S_{21}(f_k)$. The measured resonance curve can be expressed as

$$T_m(f_k) = [g(f_k) + e_{g_k}]^2 + [h(f_k) + e_{h_k}]^2 \tag{23}$$

where $g(f_k) = \Re[S_{21}(f_k)]$ and $h(f_k) = \Im[S_{21}(f_k)]$. The measured real and imaginary components of $T_m(f_k)$ are assumed to be statistically independent realizations of the same Gaussian process that has an expected value of 0 and variance σ^2. Thus, at the kth frequency, the expected value of $T_m(f_k)$ is

$$E[T_m(f_k)] = g^2(f_k) + h^2(f_k) + 2\sigma^2 \tag{24}$$

and the variance of $T_m(f_k)$ is

$$\mathrm{VAR}[T_m(f_k)] = 4\sigma^2[g^2(f_k) + h^2(f_k)] + 8\sigma^4. \tag{25}$$

Since $T(f_k) = g(f_k)^2 + h(f_k)^2$, then

$$E[T_m(f_k)] = T(f_k) + 2\sigma^2 \tag{26}$$

and

$$\mathrm{VAR}[T_m(f_k)] = 4\sigma^2 T(f_k) + 8\sigma^4. \tag{27}$$

For this special case, (26) and (27) are consistent with (13) and (14) as

$$E[T_m(f_k)] = T(f_k) + \mathrm{BG} \tag{28}$$

and

$$\mathrm{VAR}[T_m(f_k)] = \frac{\gamma_1^2}{1 + Q^2\left(\frac{f_k}{f_0} - \frac{f_0}{f_k}\right)^2} + \gamma_2^2 \tag{29}$$

where

$$\mathrm{BG} = 2\sigma^2$$
$$\gamma_1^2 = 4\sigma^2 T(f_0)$$

and

$$\gamma_2^2 = 8\sigma^4.$$

REFERENCES

[1] A. J. Estin and M. D. Janezic, "Improvements in dielectric measurements with a resonance cavity," in *Proc. 8th IEEE Instrumentation and Measurement Technology Conf.*, 1991, pp. 573–579.

[2] T. Miura, T. Takahashi, and M. Kobayashi, "Accurate q-factor evaluation by resonance curve area methods and its applications to the cavity perturbation," *IEICE Trans. Electron.*, vol. 6, pp. 900–907, 1994.

[3] P. J. Petersan and S. M. Anlage, "Measurement of resonant frequency and quality factor of microwave resonators: Comparison of methods," *J. Appl. Phys.*, vol. 84, no. 5, pp. 3392–3402, 1998.

[4] M. Davidian and R. J. Carroll, "Variance function estimation," *J. Amer. Stat. Assoc.*, vol. 82, no. 400, pp. 1079–1092, 1987.

[5] E. L. Ginzton, *Microwave Measurements*. New York: McGraw-Hill, 1957.

[6] C. G. Montgomery, R. H. Dicke, and E. M. Purcell, *Principles of Microwave Circuits*. New York: McGraw-Hill, 1974.

[7] D. Kajfez, "Q factor," in *Vector Fields*. Oxford, MS: Oxford, 1994.

[8] Y. Bard, *Nonlinear Parameter Estimation*. New York: Academic, 1974.

[9] D. M. Gay, "Computing optimal locally constrained steps," *SIAM J. Sci. Stat. Comput.*, vol. 2, pp. 186–197, 1981.

[10] R. J. Cook, "Microwave cavity methods," in *High Frequency Dielectric Measurement*, J. Chamberlain and G. W. Chantry, Eds. Guildford, U.K.: IPC Sci. Technol. Press, 1973, pp. 12–27.

[11] E. Ni and U. Stumper, "Permittivity measurements using a frequency-tuned microwave TE_{01} cavity resonator," in *Proc. Inst. Elect. Eng.*, vol. 132, Feb. 1985, pp. 27–32.

Kevin J. Coakley received the Ph.D. degree in statistics from Stanford University, Stanford, CA, in 1989.

He is currently a Mathematical Statistician with the National Institute of Standards and Technology, Boulder, CO. His research interests include statistical signal processing, computer intensive statistical methods, and planning and analysis of experiments in physical science and engineering.

Jolene D. Splett received the B.S. degree in mathematics/statistics and the M.S. degree in statistics from the University of Wyoming, Laramie.

She is a Mathematical Statistician with the Statistical Engineering Division, National Institute of Standards and Technology (NIST), Boulder, CO, where her primary duty is to provide general statistical support for the scientists and engineers of NIST.

Michael D. Janezic (M'91–SM'02) received the B.S. and M.S. degrees in electrical engineering from the University of Colorado at Boulder, in 1991 and 1996, respectively, and is currently working toward the Ph.D. degree in electrical engineering in the area of electromagnetic theory at the University of Colorado at Boulder.

In 1988, he joined the Radio Frequency Technology Division, National Institute of Standards and Technology (NIST), Boulder, where he has primarily focused on the development of techniques for measuring the broad-band electrical properties of dielectric substrates and thin films.

Raian F. Kaiser received the B.S.-E.E./C.S. degree from the University of Colorado at Boulder, in 1986.

She is currently with the Electromagnetic Properties of Materials Group, National Institute of Standards and Technology, Boulder, CO.